forests

MDPI

Article

Wall-to-Wall Mapping of Forest Biomass and Wood Volume Increment in Italy

Francesca Giannetti [1], Gherardo Chirici [1,2], Elia Vangi [1,3,4,*], Piermaria Corona [5,6], Fabio Maselli [7], Marta Chiesi [7], Giovanni D'Amico [1,6] and Nicola Puletti [6]

1 geoLAB—Laboratory of Forest Geomatics, Department of Agricultural, Food, Environmental and Forestry Sciences and Technologies, University of Florence, 50145 Firenze, Italy
2 Fondazione per il Futuro delle Città, 50133 Firenze, Italy
3 Department of Bioscience and Territory, University of Molise, 86100 Campobasso, Italy
4 Forest Modelling Laboratory, Institute for Agriculture and Forestry Systems in Mediterranean, National Research Council of Italy (CNR-ISAFOM), Via Madinna Alta 128, 06128 Perugia, Italy
5 Department for Innovation in Biological, Agri-Food and Forestry Systems, University of Tuscia, 01100 Viterbo, Italy
6 Council for Agricultural Research and Economics, Research Centre for Forestry and Wood (CREA), 52100 Arezzo, Italy
7 Italian National Research Council—Institute of BioEconomy (CNR-IBE), Via Madonna del Piano 10, 50019 Sesto Fiorentino, Italy
* Correspondence: elia.vangi@unifi.it

Abstract: Several political initiatives aim to achieve net-zero emissions by the middle of the twenty-first century. In this context, forests are crucial as a carbon sink to store unavoidable emissions. Assessing the carbon sequestration potential of forest ecosystems is pivotal to the availability of accurate forest variable estimates for supporting international reporting and appropriate forest management strategies. Spatially explicit estimates are even more important for Mediterranean countries such as Italy, where the capacity of forests to act as sinks is decreasing due to climate change. This study aimed to develop a spatial approach to obtain high-resolution maps of Italian forest above-ground biomass (ITA-BIO) and current annual volume increment (ITA-CAI), based on remotely sensed and meteorological data. The ITA-BIO estimates were compared with those obtained with two available biomass maps developed in the framework of two international projects (i.e., the Joint Research Center and the European Space Agency biomass maps, namely, JRC-BIO and ESA-BIO). The estimates from ITA-BIO, JRC-BIO, ESA-BIO, and ITA-CAI were compared with the 2nd Italian NFI (INFC) official estimates at regional level (NUT2). The estimates from ITA-BIO are in good agreement with the INFC estimates (R^2 = 0.95, mean difference = 3.8 t ha^{-1}), while for JRC-BIO and ESA-BIO, the estimates show R^2 of 0.90 and 0.70, respectively, and mean differences of 13.5 and of 21.8 t ha^{-1} with respect to the INFC estimates. ITA-CAI estimates are also in good agreement with the INFC estimates (R^2 = 0.93), even if they tend to be slightly biased. The produced maps are hosted on a web-based forest resources management Decision Support System developed under the project AGRIDIGIT (ForestView) and represent a key element in supporting the new Green Deal in Italy, the European Forest Strategy 2030 and the Italian Forest Strategy.

Keywords: forest biomass; National Forest Inventories; remote sensing; Mediterranean forest; forest increment

check for updates

Citation: Giannetti, F.; Chirici, G.; Vangi, E.; Corona, P.; Maselli, F.; Chiesi, M.; D'Amico, G.; Puletti, N. Wall-to-Wall Mapping of Forest Biomass and Wood Volume Increment in Italy. *Forests* **2022**, *13*, 1989. https://doi.org/10.3390/f13121989

Academic Editor: Dmitry Schepaschenko

Received: 30 September 2022
Accepted: 20 November 2022
Published: 24 November 2022

1. Introduction

Measuring the amount of CO_2 stocked in forest ecosystems is mandatory to support the new European (EU) Forest Strategy for 2030, a flagship initiative of the European Green Deal, in sight of achieving neutrality with respect to greenhouse gas emission in 2050 [1,2]. In this context, the estimation of forest biomass is pivotal to evaluate the carbon sequestration potential of forest ecosystems [3–5].

As reported by Ruiz-Peinado et al. [3], the assessment of carbon balance and carbon sink is critical in Mediterranean areas, where in the last years, the capacity of forests to act as sinks is decreasing due to the climate change (e.g., hot and dry summers, irregular precipitations, increasing temperatures) and to the increasing frequency of extreme forest disturbances [4,6]. For example, Vayreda et al. [7] underline that climate change is causing a reduction in the carbon sink capacity of unmanaged Spanish forests due to the lower water availability. For these reasons, national-level accurate estimations of forest biomass and carbon fluxes are also critical to support sustainable forest management and specific silvicultural systems that can help the maintenance of carbon sink [3,5] under an evidence-based framework [8].

At EU scale, various maps of forest biomass are available [9], such as those by Thurner et al. [10], Barredo et al. [11], Gallaun et al. [12], Kindermann et al. [13], Baccini et al. [14], and Santoro [15]. However, as stressed by the Joint Research Center (JRC) in 2020 [16], the mentioned maps show high relative mean square error (RMSE) ranging from 29% to 40% at the national level. JRC has deemed such maps unreliable and, in 2020, developed a forest biomass map (JRC-BIO) in line with the statistics of National Forest Inventories (NFIs): this map has a 100 m $\times$ 100 m spatial resolution, was constructed applying a bias-removal approach to the Santoro map [15], and refers to the nominal year 2010. The European Space Agency (ESA), with the aim of quantifying changes in carbon stored in forests, provided the global above-ground biomass maps (ESA-BIO) at 1 km $\times$ 1 km for the years 2010, 2017, and 2018 by exploiting synthetic aperture radar data [17].

Various authors underline that global or continental forest maps are not suitable to quantify forest variables with high accuracy at national level [18,19]. For those reasons, countries usually adopt aggregate statistics of forest biomass, growing stock volume, and volume increments derived from NFIs to estimate the CO_2 fluxes in the context of international agreements [20–23]. Aggregate statistics of the NFI enable to develop strategies over large areas but do not provide spatial details to assess the biomass and CO_2 fluxes over small areas [23]; so, they are unable to support sustainable forest management [24].

The spatial detail over small areas can be achieved moving from conventional NFIs to Enhanced Forest Inventories (EFIs) [25] that, by integrating NFI plot measurements with remote sensing data, can provide estimates of forest variables, such as growing stock volume (GSV) [23,26–31], annual volume increments [32–34], and biomass [29,31], at various spatial scales. Such an approach enables to analyze changes over spatial scales, from national to small scale [23,24], and the information from EFIs can be used for multiple purposes such as to support sustainable management of forest estates by implementing the maps in Forest Information Systems (FIS) and/or in Decision Support System (DSS), besides designing forest management policy strategies.

The main difference between maps developed at global/continental level and those developed in the context of EFIs is the spatial scale. The forest resource maps developed in the context of EFIs are produced at a fine spatial resolution ($\leq$30 m $\times$ 30 m), which is consistent with the size of the field sampling units and can be used to implement operational FIS and DSS.

The EFI approach is well established in many North [24] and Central Europe Countries (e.g., Switzerland [35] and Germany [36]), while in the EU Mediterranean ones only few examples are available (Spain: Novo-Fernández et al. [37]; Italy: Chirici et al. [23], Vangi et al. [26], Chirici et al. [32]; Greece: Chrysafis et al. [38,39]).

In Spain, Novo-Fernández et al. [37] and Pascual et al. [40] demonstrated that the NFI plots can be coupled with Airborne Laser Scanning (ALS) to obtain accurate GSV estimates, underlining that Spanish conventional NFI might be transformed to ALS-based NFI. Researches conducted in Italy on both broadleaved and coniferous forests with ALS show that GSV can be predicted at stand level with suitable precision [41–43]. However, Italy has no wall-to-wall ALS data coverage [18]; so, various authors have investigated the potential of using satellite data coupled with NFI plot data for predicting forest variables wall-to-wall. Chirici et al. [23] and Vangi et al. [26] showed that GSV can be predicted

at fine spatial scale (23 m × 23 m) using Landsat and auxiliary variables (e.g., climate and orographic). Chirici et al. [32] demonstrated also that, using NFI data, Moderate Resolution Imaging Spectroradiometer (MODIS), ancillary data, and the wall-to-wall GSV map [23] allows mapping the current annual increment (CAI) in Tuscany Region at a scale of 23 m × 23 m by integrating two ecophysiologically-based models (C-Fix and BIOME-BGC).

Forests in Italy are the largest terrestrial ecosystems, covering more than 11 million ha (37% of Italian land). Italian forests contain more than 569 million of tons of organic carbon above ground [44]. It is mandatory to set up a methodology to develop the Italian forest variables maps, which provides spatially explicit estimates of biomass and annual increment. Since plot measurements from the last Italian NFI (hereafter called INFC) are not yet available [44,45], we developed the methodology here presented by using the plot data from 2005.

This paper is aimed at the following: (i) illustrating the developed methodology to elaborate wall-to-wall forest biomass and CAI maps of Italy (i.e., the ITA-BIO and ITA-CAI maps); (ii) comparing the biomass estimates derived from ITA-BIO with those obtained from INFC and from JRC-BIO and ESA-BIO; (iii) combining the INFC biomass and CAI field observations with the ITA-BIO and ITA-CAI maps to produce model-assisted estimates of biomass and CAI at the sub-national level.

2. Materials and Methods

2.1. Study Area

Italy covers over 301,000 km^2 and is divided into 21 local administrative Regions (NUT2) and 107 administrative territorial lands (NUT3) following the European Statistical Office classification (Eurostat). The Italian territory is characterized by large geographical and topographical variability, from coastal areas to gentle hills and steep mountains. Even the climate is characterized by high variability, mostly influenced by the distance from the sea (Mediterranean basin) and the elevation (up to about 4800 m asl).

According to INFC, forest vegetation is characterized by deciduous broadleaves (68%), mainly *Quercus* spp. (*Q. petrea* M., *Q. pubescens* W., *Q. robur* L., *Q. cerris* L.) and *Fagus sylvatica* L., while the dominant conifers are *Picea abies* Karst, especially in the Alpine regions, and *Pinus* spp. (*Pinus sylvestris* L., *P. nigra* Arnold, *P. pinae* L., *P. pinaster* Ait). According to the European Forest Types classification system [46,47], 7 of the 14 EU Forest Types classes occur in Italy.

2.2. Data

2.2.1. Italian National Forest Map

To develop the wall-to-wall ITA-BIO map, the wall-to-wall GSV map of Italy developed by Vangi et al. (2021) [26] was exploited as input data (Figure 1). The GSV map was produced by applying the Random Forest algorithm to INFC field observations and several environmental (e.g., topographic, climatic, land cover and soil maps, bioregions) and satellite predictors (e.g., Landsat bands, Global PALSAR/PALSAR-2 bands). The Italian GSV map is a 23 m × 23 m raster grid that provides, for each pixel, the GSV expressed in m^{3}ha^{-1}. More details can be found in Chirici et al. [23] and Vangi et al. [26].

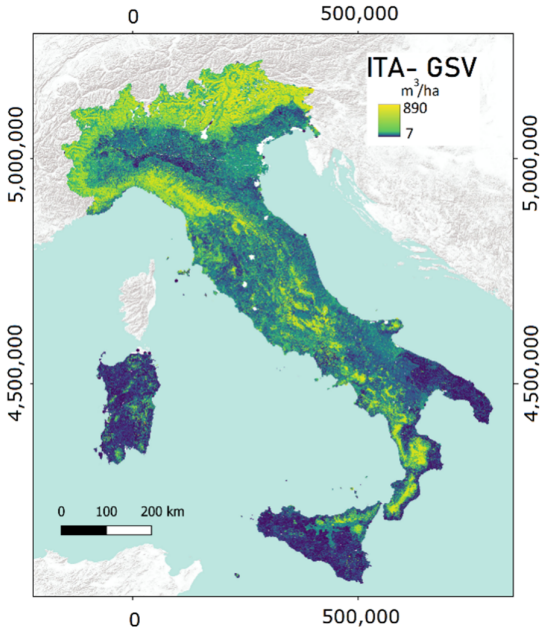

Figure 1. Italian National Growing Stock Map with a resolution of 23 m × 23 m [26].

2.2.2. Corine Land Cover Forest Types, Biomass Expansion Factors, and Wood Basic Densities

To convert the GSV into biomass, two key information are needed: (i) spatial distribution of forest types; (ii) biomass expansion factors (BEFs) and wood basic densities (WBDs) for each forest type.

Since a forest type map covering the whole national territory is not available for Italy [18], we decided to use the CORINE Land Cover (CLC) at IV level (Table 1). More specifically, we used the CLC IV level database of 2006 [48], having a nominal scale 1:100,000 and a minimum mapping unit of 25 ha. We rasterized the vector maps with a spatial resolution of 23 m × 23 m, consistent with the GSV map and the national grid developed by D'Amico et al. [18]. The obtained raster grid CLC Forest Types map was then masked with the Italian forest mask developed by D'Amico et al. [18] to delete non-forest areas.

Table 1. Nomenclature system of Corine Land Cover (IV Level) forest types, biomass expansion factors (BEF), and wood basic densities (WBD) based on Federici et al. [49].

CLC IV Forest Types Nomenclature Systems	BEF (Volume of Aboveground Biomass/ Volume of Growing Stock)	WBD (Dry Weight t/ Fresh Volume of Aboveground Biomass m^3)
3.1.1.1. Forest dominated by holm oak and/or cork oak	1.45	0.72
3.1.1.2. Forest dominated by deciduous oak (Turkey oak, downy oak, farnetto oak, and/or English oak)	1.39	0.65
3.1.1.3. Mixed forests with a prevalence of mesophilic and mesothermophilous broad-leaved trees (maple-ash, cute black-ash)	1.28	0.66
3.1.1.4. Chestnut forests	1.33	0.49
3.1.1.5. Beech forests	1.36	0.61
3.1.1.6. Forests dominated by hygrophilous species (forests with a prevalence of willows, poplars, and/or alders, etc.)	1.39	0.41
3.1.2.1. Forests dominated by Mediterranean pines (stone pine, pine maritime) and cypress	1.53	0.53
3.1.2.2. Forests dominated by mountain and Mediterranean pines (black pine and larch, Scots pine, Bosnian pine)	1.33	0.47
3.1.2.3. Forests dominated by silver fir and/or spruce	1.34	0.38
3.1.2.5. Forests dominated by larch and/or stone pine	1.37	0.43
3.1.3.1 Mixed Forests with a prevalence of broad-leaved trees	1.53	0.53
3.1.3.2 Mixed Forests with a prevalence of conifers	1.37	0.43

Then, for each CLC forest type, we derived the BEF and the WBD (Table 1) calculated as the mean of the species present in each CLC forest type based on Federici et al. [49].

2.2.3. Biomass Maps from International Frameworks

As mentioned, we compared the ITA-BIO map here developed (Section 3) with two products, JRC-BIO and ESA-BIO maps, which represent the most accurate maps available for the Italian territory and refer to a nominal year (the 2010) closer to that of the INFC data here used (the field survey of INFC finished in 2008, and, as underlined by McRoberts et al. [50], two years of discrepancy should have minor impact on the comparison).

Both ESA-BIO and JRC-BIO, which provide above-ground biomass expressed in t ha^{-1}, were masked with the Italian forest mask developed by D'Amico et al. [18] to delete non-forest area and to obtain products that are comparable with the one here developed.

2.2.4. Field Italian National Forest Inventory Plot Data

The field reference data were measured within 6782 plots surveyed in the framework of the INFC [51]. The available plot geolocation has been the target coordinate of the sampling unit. For each field plot, the biomass per hectare derived using the allometric equation developed by Tabacchi et al. [52] and the CAI (m^3 ha^{-1}) are available online via a spatial database at https://www.inventarioforestale.org/ (accessed on 1 March 2021) [53]. Figure 2 shows the spatial distribution of the plots and the biomass measured in the field. For more details about INFC, we refer to Chirici et al. [23].

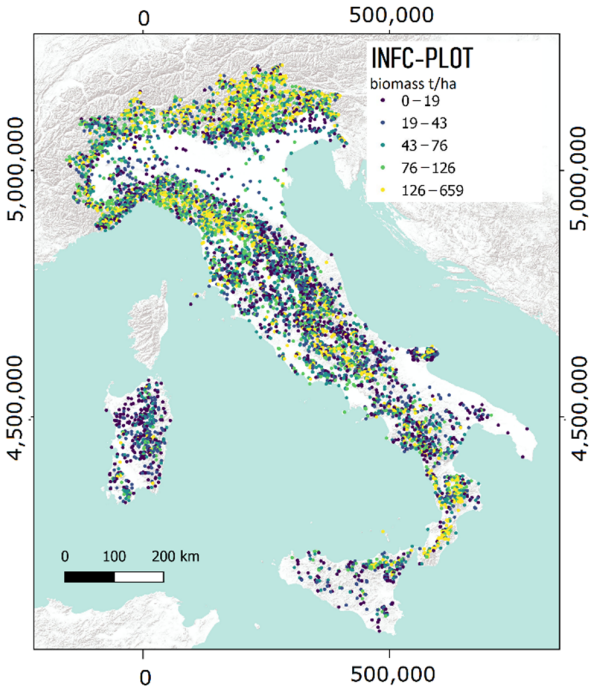

Figure 2. Spatial distribution of INFC plots with respective biomass classes [54].

2.3. Methods

2.3.1. Wall-to-Wall Forest Biomass Map

The GSV data were converted into biomass (BIO) following Federici et al. [49]:

$$BIO = GSV \cdot BEF \cdot WDB \quad (1)$$

where GSV is the pixel value of growing stock volume (m^3 ha^{-1}), BEF is the biomass expansion factor of each CLC forest type, and WBD is the wood basic density of each CLC forest type (Table 1).

The obtained biomass map (ITA-BIO) has pixels of 23 m × 23 m reporting the forest biomass in t ha^{-1}.

2.3.2. Model-Assisted Estimation

To construct an inference for the mean value of biomass for a given survey area from the ITA-BIO, JRC-BIO, and ESA-BIO maps, the model-assisted estimation approach was adopted, exploiting the biomass measured in the 6782 INFC field plots as proposed by Chirici et al. [23].

The map-based estimate of the mean biomass in a given forest area is

$$\hat{\mu}_{map} = \frac{1}{N} \sum_{j=1}^{N} \hat{y}_i \quad (2)$$

where N is the number of map units (23 m × 23 m pixels) in the area and $\hat{y}_i$ is the biomass of each map unit.

Then, the map-based estimate is adjusted for systematic errors by bias estimation calculated as

$$\widehat{Bias}\left(\hat{\mu}_{map}\right) = \frac{1}{n} \sum_{i=1}^{n} (\hat{y}_i - y_i) \quad (3)$$

where n is the number of INFC plots in the area, y_i is the biomass measured in the i-th INFC plot, and $\hat{y}_i$ is the biomass predicted for the corresponding map unit.

The model-assisted estimate is the map estimate with the estimated bias subtracted:

$$\hat{\mu}_{model\text{-}assisted} = \hat{\mu}_{map} - \hat{Bias}\left(\hat{\mu}_{map}\right) \quad (4)$$

while the standard error (SE) of $\hat{\mu}_{model\text{-}assisted}$ is

$$SE(\hat{\mu}_{model\text{-}assisted}) = \sqrt{\frac{1}{n(n-1)} \sum_{i=1}^{n} (e_i - \bar{e})^2} \quad (5)$$

where $e_i = (\hat{y}_i - y_i)$ and $\bar{e} = \frac{1}{n} \sum_{i=1}^{n} e_i$.

2.3.3. Accuracy Assessment

To assess the accuracy of ITA-BIO, JRC-BIO, and ESA-BIO maps, we compared the $\hat{\mu}_{model\text{-}assisted}$ biomass estimates with the INFC biomass statistics at NUT2 level (i.e., regional level) freely available online at https://www.sian.it/inventarioforestale (accessed on 1 March 2021) (Table 2).

We calculated the coefficient of determination (R^2) for each NUT2 between official NFI estimates and $\hat{\mu}_{model\text{-}assisted}$.

Table 2. $\hat{\mu}_{NFI}$ and $\hat{\mu}_{model\text{-}assisted}$ (with respective standard errors, SE) for the three considered biomass maps (ITA-BIO, JRC-BIO, ESA-BIO) at NUT2 level.

	INFC-BIO		ITA-BIO		JRC-BIO		ESA-BIO	
Region (NUT2)	$\hat{\mu}_{NFI}$ **t ha^{-1}**	**SE (%)**	$\hat{\mu}_{model\text{-}assisted}$ **t ha^{-1}**	**SE t ha^{-1}**	$\hat{\mu}_{model\text{-}assisted}$ **t ha^{-1}**	**SE t ha^{-1}**	$\hat{\mu}_{model\text{-}assisted}$ **t ha^{-1}**	**SE t ha^{-1}**
Abruzzo	77.7	4.5	75.2	2.37	55.7	4.88	50.1	4.84
Alto Adige	130.5	4.3	123.9	3.96	116.7	7.69	106.1	6.18
Basilicata	64.3	6.7	53.0	2.83	46.6	5.54	39.4	5.66
Calabria	98.9	4.5	80.7	3.11	52.2	5.21	50.9	5.78
Campania	65.3	6	64.5	2.90	51.8	5.76	42.6	5.67
Emilia Romagna	73.5	3.6	70.8	2.32	64.2	4.31	52.3	3.99
Friuli-Venezia Giulia	107.7	4.9	114.9	3.64	101.0	7.45	98.8	6.26
Lazio	63.7	4.5	62.9	2.12	48.5	4.51	41.6	3.94
Liguria	77.5	4.2	72.5	2.60	69.5	4.66	57.7	3.99
Lombardia	86.7	3.8	83.7	2.33	74.3	5.76	71.6	3.96
Marche	48	6.4	49.8	2.23	29.9	5.49	30.5	4.47
Molise	67.6	8.7	56.8	4.72	50.3	6.54	42.1	6.32
Piemonte	77.4	2.8	78.5	1.98	65.7	4.16	56.8	3.09
Puglia	49.2	10.7	44.5	4.28	53.8	7.42	35.9	8.06
Sardegna	37.8	5.3	27.0	1.68	28.5	2.82	16.8	3.47
Sicilia	50.4	6	34.8	2.55	15.8	4.54	14.3	3.84
Toscana	72.6	2.8	72.4	1.70	59.7	3.47	53.6	2.89
Trentino	122.2	4.3	123.7	3.71	115.5	7.33	108.5	5.99
Umbria	48.3	4.7	48.5	1.91	42.7	4.41	34.0	2.96
Valle d'Aosta	68.3	6.9	67.3	4.63	65.0	9.91	46.0	5.68
Veneto	98.3	4	98.8	2.82	93.4	6.22	78.3	4.31

2.3.4. CAI Modeling

The information used to produce the ITA-BIO map was coupled with meteorological datasets to derive a wall-to-wall simulation of forest CAI. Below, the main methodological steps are summarized: a detailed description of the modeling strategy is reported by Maselli et al. [55] and Chirici et al. [56], along with all the input data and the adopted assumptions.

The strategy is based on the combination of two models, C-Fix and BIOME-BGC, which simulate the gross and net carbon fluxes of forest ecosystems. The estimates produced by the two models are combined and corrected to account for the effects of natural and human-induced disturbances affecting forest ecosystems. This is achieved including an indicator of the distance from ecosystem equilibrium computed as the ratio between the actual (measured or estimated) and potential (simulated by BIOME-BGC) GSV: the ratio is used to correct the photosynthesis and respiration estimates obtained by the model simulations [56], computing actual NPP (NPP_A) as

$$NPP_A = GPP \cdot FC_A - Rgr \cdot FC_A - Rmn \cdot NV_A \quad (6)$$

where GPP, Rgr, and Rmn are the BIOME-BGC estimates of photosynthesis, growth, and maintenance respirations, corrected for the GPP simulated by C-Fix; and the two terms FC_A (actual forest cover) and NV_A (actual normalized volume) describe the ecosystem proximity to the equilibrium condition [53]. Distinctively, NV_A is the mentioned ratio between the actual and potential GSV, and FC_A represents the fraction of photosynthetic radiation usable by the tree canopy, obtained by combining NV_A and the leaf area index (LAI) following Beer's law.

Finally, NPP_A can be converted into CAI by the following formula [38]:

$$CAI = NPP_A \cdot (SCA/BEF/BWD) \cdot 2/100 \quad (7)$$

where SCA is the stem carbon allocation ratio, defined for each forest type by BIOME-BGC, while the values of BEF and BWD are taken again from Federici et al. [50]. The multiplication by 2 accounts for the conversion from carbon to dry matter, and the division by 100 for the change in magnitude from g m^{-2} to Mg ha^{-1}.

Equations (6) and (7) were applied to yield the ITA-CAI map with a pixel size of 250 m for all Italian forests. The accuracy of this map was assessed against the INFC CAI estimates at NUT2 level (i.e., regional level) freely available online at https://www.sian.it/inventarioforestale (accessed on 1 March 2021).

3. Results

The ITA-BIO map is shown in Figure 3. The main patterns of Figure 2 are well reproduced, with the lowest biomass values found in Sardinia and the highest on the Alps, particularly in the north-east.

Table 2 reports the mean biomass values and the corresponding standard errors for the Italian regions (NUT2), both derived from the INFC official statistics ($\hat{\mu}_{NFI}$) and from the map produced here ($\hat{\mu}_{model\text{-}assisted}$ of ITA-BIO). In addition, there are the corresponding values derived from the other two maps, ESA-BIO and JRC-BIO, for comparison. All three maps provide comparable results both in terms of mean and standard error. The coefficient of determination (R^2) between the means from the considered maps and $\hat{\mu}_{NFI}$ is greater than 0.70 (ITA-BIO = 0.95, ESA-BIO = 0.70, JRC-BIO = 0.90); underestimation is less evident for ITA-BIO with respect to the other two maps (Figure 4). The standard error of ITA-BIO is smaller than those of the two other biomass maps and ranges between 1.68 t ha^{-1} in Toscana and Sardegna and 4.72 t ha^{-1} in Molise (Table 2). The lowest differences in terms of $\hat{\mu}_{NFI}$ and $\hat{\mu}_{model\text{-}assisted}$ for ITA-BIO are observed in Toscana (0.2 t ha^{-1}), Umbria (-0.2 t ha^{-1}), Veneto (-0.5 t ha^{-1}), Campania and Lazio (0.8 t ha^{-1}), Valle d'Aosta (1 t ha^{-1}), and Piemonte (-1.1 t ha^{-1}), while larger differences are observed in Calabria (18.2 t ha^{-1}), Sicilia (15.6 t ha^{-1}), Basilicata (11.3 t ha^{-1}), Sardegna and Molise (10.8 t ha^{-1}), and Friuli-Venezia Giulia (-7.2 t ha^{-1}). ESA-BIO and JRC-BIO show the greatest differences between $\hat{\mu}_{model\text{-}assisted}$ and $\hat{\mu}_{NFI}$ for Calabria (ESA-BIO: 46.7 t ha^{-1}; JRC-BIO: 48 t ha^{-1}), Sicilia (ESA-BIO: 34.6 t ha^{-1}; JRC-BIO: 36.1 t ha^{-1}), and Basilicata (ESA-BIO: 17.7 t ha^{-1}; JRC-BIO: 24.9 t ha^{-1}). In terms of differences between $\hat{\mu}_{NFI}$ and $\hat{\mu}_{model\text{-}assisted}$, JRC-BIO performs slightly better than ITA-BIO in Friuli-Venezia Giulia (JRC-BIO: 6.7 t ha^{-1}; ITA-BIO: -7.2 t ha^{-1}), while in Puglia both maps produce comparable results (JRC-BIO: -4.6 t ha^{-1}; ITA-BIO: 4.7 t ha^{-1}), with JRC-BIO overestimating and ITA-BIO underestimating the mean biomass. Regarding ESA-BIO, relevant differences between $\hat{\mu}_{NFI}$ and $\hat{\mu}_{model\text{-}assisted}$ are observed, ranging between 8.9 t ha^{-1} in Friuli Venezia Giulia and 48 t ha^{-1} in Calabria. ITA-BIO tends to slightly overestimate the mean biomass in Umbria, Veneto, Piemonte, Trentino, and Marche, while underestimation is observed for all other regions. JRC-BIO and ESA-BIO underestimate the mean biomass in all regions except for JRC-BIO in Puglia.

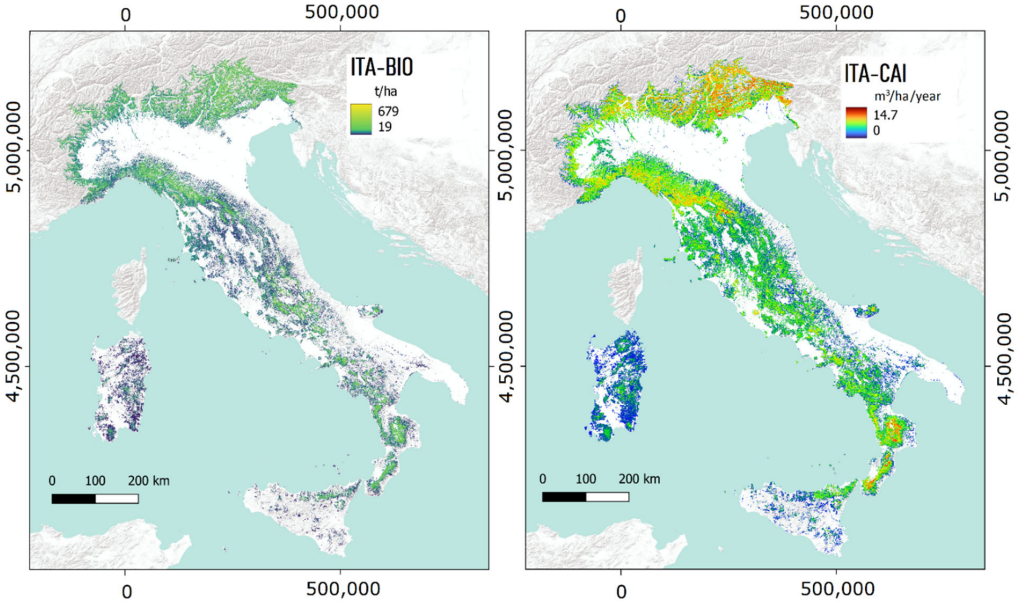

Figure 3. ITA-BIO map (**left**) and ITA-CAI map (**right**) obtained at the nominal year of 2005.

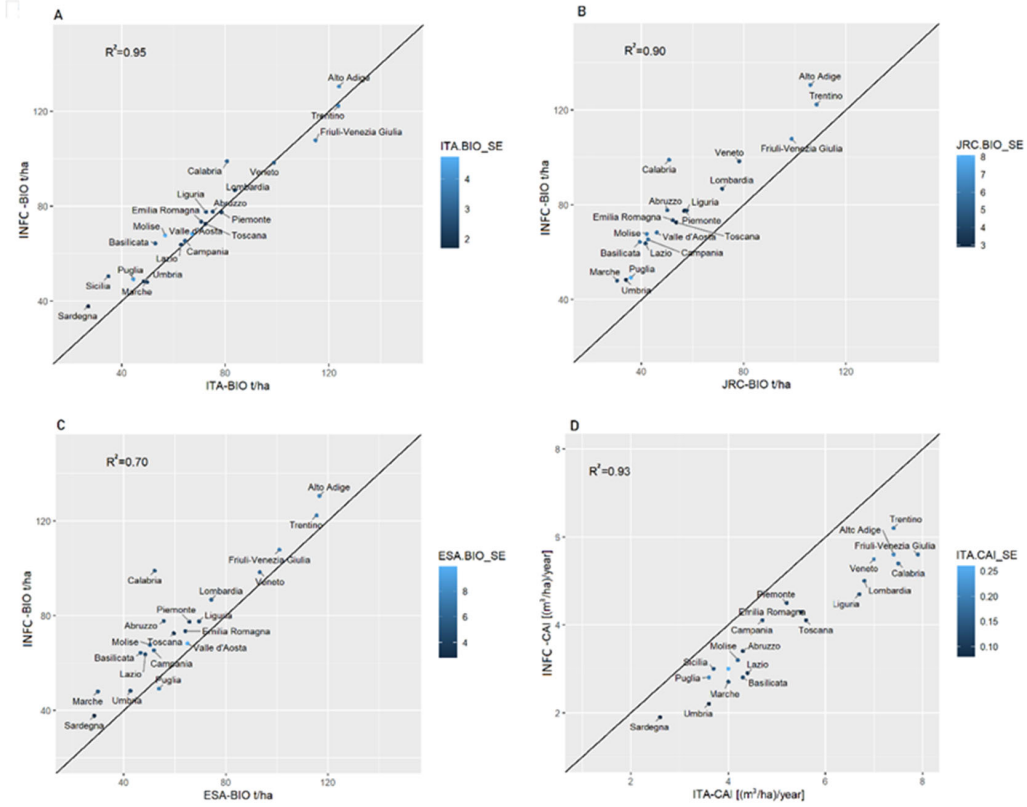

Figure 4. (**A**–**C**) $\hat{\mu}_{model\text{-}assisted}$ from the three biomass maps at NUT2 level (**A**: ITA-BIO, **B**: ESA-BIO, **C**: JRC-BIO) against $\hat{\mu}_{NFI}$, with the black line being the 1:1 line. The biomass unit is t ha^{-1}. (**D**) $\hat{\mu}_{model\text{-}assisted}$ of CAI map against $\hat{\mu}_{NFI}$. The black line is the 1:1 line. The CAI unit is m^3 ha^{-1}year^{-1}. The colors of the dots represent the standard errors (SE) derived from the maps.

The CAI variations shown in Figure 3 follow the main patterns of the forest GSV; however, some differences are also due to forest types. The ITA-CAI map at NUT2 level provides a good fit with $\hat{\mu}_{NFI}$ with R^2 equal to 0.93 (Figure 4). The CAI map is affected by relatively small standard errors, ranging between 0.26 m^3 ha^{-1} year^{-1} in Valle d'Aosta and 0.10 m^3 ha^{-1} year^{-1} in Lazio, Toscana, and Abruzzo. The ITA-CAI tends to overestimate

CAI in all regions with respect to INFC (Table 3 and Figure 4). The smallest CAI differences between $\hat{\mu}_{NFI}$ and $\hat{\mu}_{model\text{-}assisted}$ are observed in Campania (-0.6 m^3 ha^{-1} year^{-1}), Sicilia, Sardegna, and Piemonte (-0.7 m^3 ha^{-1} year^{-1}), while the greatest ones are found in Friuli Venezia-Giulia (-2.3 m^3 ha^{-1} year^{-1}), Calabria (-2.1 m^3 ha^{-1} year^{-1}), Liguria (2 m^3 ha^{-1} year^{-1}), Alto Adige, and Lombardia (-1.8 m^3 ha^{-1} year^{-1}). For all other regions, the CAI differences range between -1.5 m^3 ha^{-1} year^{-1} and -0.9 m^3 ha^{-1} year^{-1} (Table 3 and Figure 4).

Table 3. $\hat{\mu}_{NFI}$ and $\hat{\mu}_{model\text{-}assisted}$ (with respective standard errors, SE) for the ITA-CAI map at NUT2 level.

	INFC-CAI		ITA-CAI	
Region (NUT2)	$\hat{\mu}_{NFI}$ **m^{3}ha^{-1}year^{-1}**	**SE (%)**	$\hat{\mu}_{model-assisted}$ **m^{3}ha^{-1}year^{-1}**	**SE m^{3}ha^{-1}year^{-1}**
Abruzzo	3.4	4.5	4.3	0.10
Alto Adige	5.6	4.0	7.4	0.21
Basilicata	2.8	5.5	4.3	0.13
Calabria	5.4	4.4	7.5	0.17
Campania	4.1	5.1	4.7	0.13
Emilia Romagna	4.3	3.7	5.5	0.11
Friuli-Venezia Giulia	5.6	4.5	7.9	0.17
Lazio	2.9	4.6	4.4	0.10
Liguria	4.7	4.6	6.7	0.13
Lombardia	5.0	3.6	6.8	0.15
Marche	2.7	7.0	4.0	0.13
Molise	3.2	7.0	4.2	0.16
Piemonte	4.5	3.1	5.2	0.12
Puglia	2.8	8.2	3.6	0.21
Sardegna	1.9	5.2	2.6	0.08
Sicilia	3.0	6.5	3.7	0.14
Toscana	4.1	3.3	5.6	0.10
Trentino	6.2	4.0	7.4	0.19
Umbria	2.2	4.6	3.6	0.08
Valle d'Aosta	3.0	7.4	4.0	0.26
Veneto	5.5	3.7	7.0	0.20

4. Discussion and Conclusions

The main objective of the study was to develop a spatial approach to obtain both the 23 m × 23 m forest biomass map (ITA-BIO) and the CAI map (ITA-CAI) of Italy. The proposed approach allows derivation of estimates at various spatial scales with associated uncertainty as required by the reporting under international environmental agreements.

The model-assisted estimates based on the ITA-BIO map reduce the error of INFC estimates at the regional level (Table 2), which is also lower than model-assisted estimates based on other available biomass maps. Both the JRC-BIO and the ESA-BIO underestimate the mean forest biomass ($\hat{\mu}_{model\text{-}assisted}$) (with the only exception of JRC-BIO for Puglia region) compared with the INFC estimate (mean difference = 13.5 and 21.8 t ha^{-1} for JRC-BIO and ESA-BIO, respectively), while ITA-BIO is characterized by a small mean difference (3.8 t ha^{-1}) (Table 2, Figure 4). The results regarding JRC-BIO and ESA-BIO maps are in disagreement with those found by Neeti in the USA [57], since we found that these maps underestimate the mean biomass with respect to INFC. Comparing four different global biomass products, Araza et al. [58] showed a disagreement between their mean values in most of the regions, where we observed the largest differences between $\hat{\mu}_{NFI}$ and $\hat{\mu}_{model\text{-}assisted}$ for ITA-BIO, JRC-BIO, and ESA-BIO (i.e., Calabria, Sicilia, Abruzzo, Marche, Molise, and Basilicata) (Table 2). In the mentioned regions, the standard errors of INFC are also the highest.

As pointed out by Zhang et al. [59] and Huang [60], the inconsistency between biomass maps observed in our study can be attributed to the allometric equations used to compute field data, to the choice and quality of remotely sensed data, as well as to the algorithms for mapping forest biomass or to the extrapolation techniques.

The more accurate results observed for ITA-BIO with respect to JRC-BIO and ESA-BIO are due to the fact that our approach was distinctively calibrated for the Italian forests, allowing to reach higher reliability, as observed by previous studies investigating other forest variables such as forest area [18] and forest disturbance area [19,61].

However, the results obtained by all three biomass maps in terms of R^2 and mean biomass estimates at coarse scales (e.g., regional level) are in line with the ones obtained in Mexico ($R^2 > 0.66$) using a calibration approach with LiDAR, NFI, satellite remote sensing (i.e., ALOS PALOSAR and Landsat) data, and a machine learning approach [62], and with the results of Huang [60] in the USA and Avitabile [63] in Uganda. On the other hand, our study confirms the finding of Araza et al. [59], who demonstrated that global biomass maps, if adopted to estimate the mean biomass at coarse scales (i.e., regional level), can be effective to a certain extent. At the level of single pixels, the map may be affected by a substantial bias [59,62]; however, when aggregating several pixels to areas of increasing size (e.g., forest estates, provinces, regions), the average value tends to converge to the real value, since the model-assisted estimator is unbiased [58,61,64]. Nevertheless, it can be expected that global maps produce even larger errors than the ones obtained at regional scales when used at small spatial scales (e.g., forest stands and forest management units). In this regard, the spatial scale of ITA-BIO (23 m $\times$ 23 m) can provide more precise estimates at small scales [23] and is more suitable to support forest management compared with the other maps (1 km $\times$ 1 km for ESA map, 1 ha for JRC map) [24].

The available high-spatial-resolution forest biomass maps can be combined with other data layers to yield additional wall-to-wall forest descriptors, such as CAI. As previously noted, the CAI modeling strategy is based on the efficient combination of parametric and bio-geochemical models, C-Fix and BIOME-BGC. The former merges meteorological and NDVI data to yield forest GPP estimates [56], which are then used to improve the functioning of BIOME-BGC and simulate all Mediterranean ecosystem processes and maximum GSV. The latter term allows the calculation of the two scalars accounting for forest disturbances (NV_A and FC_A), which are decisive to simulate forest NPP_A and then derive CAI. As fully discussed in [32], this strategy does not take into consideration some factors that are important for woody biomass accumulation but cannot be properly assessed over wide areas (e.g., plant age and management condition). The simulation of CAI can be also deteriorated by the use of mapped GSV estimates and species-specific BEFs, both implying additional uncertainty [56].

The NUT2 level model-assisted estimates derived from the ITA-CAI map are in good agreement with the CAI estimates by INFC ($R^2 = 0.93$), but they show a certain tendency to overestimation (mean bias error = 1.3 $m^3 ha^{-1}$ $year^{-1}$). The reason, already stressed by Chirici et al. [56], might be prevalently due to the characteristics of the input data layers: for instance, the spatial resolution of the adopted national meteorological datasets (1 km) is not suboptimal to capture local environmental variability.

The maps presented in this paper (ITA-BIO and ITA-CAI) are hosted on a web-based forest resources management DSS developed under the project AGRIDIGIT (ForestView) and available at http://progetti.technocenter.it/crea/#/forestview. Such maps represent a key element to support the new Green Deal, the EU Forest Strategy 2030, and the Italian Forest Strategy since they can be used for multiple objectives such as to quantify biomass and sequestered CO_2, to assess the availability of wood for production and to monitor the status of forest ecosystems. This web-based DSS will include modules dedicated to forest management planning and decision making, and a graphical user interface (GUI) for relevant GIS analysis.

A weakness of the current study is that the maps produced have both a nominal year of 2005 that is not consistent with the ongoing forest management activities [24]; however,

during the study, the observations of the new 2015 INFC plots were not yet released [45]. Nevertheless, the methodology developed and tested here can be applied immediately to the new data when available. In addition, it is important to point out that the CAI map, giving the spatial explicit estimation of mean annual increment (m^3 ha^{-1} $year^{-1}$), adopted in conjunction with the forest disturbance maps (i.e., clearcut, forest fire, windstorm and developed in Italy at country/regional and local scales [19,61,64–67]), is potentially useful for yearly updating the GSV map and, consequently, the biomass map. In this regard, future research efforts integrating those maps and other increment models are expected in order to yield yearly updated spatially explicit estimates of those forest variables (i.e., GSV and biomass) useful for forest management and for the reporting of international frameworks (e.g., ICPP [20], Forest Europe [68], and Global Forest Resource Assessment [69]).

Author Contributions: Conceptualization, G.C., F.G., N.P, P.C., F.M. and M.C.; methodology, F.G., E.V., F.M. and M.C.; validation, F.G., E.V., F.M. and M.C.; formal analysis F.G., E.V., G.D. and F.M., resources, N.P.; data curation, F.G., E.V., F.M. and M.C.; writing—original draft preparation, F.G., F.M., M.C. and N.P.; writing—review and editing, E.V., G.D., G.C. and P.C. All authors have read and agreed to the published version of the manuscript.

Funding: This research was funded with the contribution of the Italian Ministry of Agriculture, Food, and Forestry Policies (MiPAAF), subproject "Precision Forestry" (AgriDigit program-DM 36503.7305.2018 of 2 December 2018).

Data Availability Statement: Data presented in this study are available on request from the corresponding author and will be published on the online DSS.

Conflicts of Interest: The authors declare no conflict of interest.

References

1. European Commission. *New EU Forest Strategy for 2030*; European Commission: Brussels, Belgium, 2021; pp. 5–24.
2. *52019DC0640*; Commission European Communication from the Commission to the European Parliament, The European Council, The Council, The European Economic and Social Committee and The Committee of the Regions The European Green Deal COM/2019/640 Final. European Commission: Brussels, Belgium, 2019.
3. Ruiz-Peinado, R.; Bravo-Oviedo, A.; López-Senespleda, E.; Bravo, F.; del Río, M. Forest management and carbon sequestration in the Mediterranean region: A review. *For. Syst.* **2017**, *26*, 2. [CrossRef]
4. Peñuelas, J.; Sardans, J. Global change and forest disturbances in the mediterranean basin: Breakthroughs, knowledge gaps, and recommendations. *Forests* **2021**, *12*, 603. [CrossRef]
5. Martes, L.; Köhl, M. Improving the Contribution of Forests to Carbon Neutrality under Different Policies—A Case Study from the Hamburg Metropolitan Area. *Sustainability* **2022**, *14*, 2088. [CrossRef]
6. Forzieri, G.; Pecchi, M.; Girardello, M.; Mauri, A.; Klaus, M.; Nikolov, C.; Rüetschi, M.; Gardiner, B.; Tomastik, J.; Small, D.; et al. A spatially explicit database of wind disturbances in European forests over the period 2000–2018. *Earth Syst. Sci. Data* **2020**, *12*, 603. [CrossRef]
7. Vayreda, J.; Martinez-Vilalta, J.; Gracia, M.; Retana, J. Recent climate changes interact with stand structure and management to determine changes in tree carbon stocks in Spanish forests. *Glob. Chang. Biol.* **2012**, *18*, 1028–1041. [CrossRef]
8. Corona, P. Communicating facts, findings and thinking to support evidence-based strategies and decisions. *Ann. Silvic. Res.* **2018**, *42*, 1. [CrossRef]
9. Avitabile, V.; Camia, A. An assessment of forest biomass maps in Europe using harmonized national statistics and inventory plots. *For. Ecol. Manage.* **2018**, *409*, 489–498. [CrossRef]
10. Thurner, M.; Beer, C.; Santoro, M.; Carvalhais, N.; Wutzler, T.; Schepaschenko, D.; Shvidenko, A.; Kompter, E.; Ahrens, B.; Levick, S.R.; et al. Carbon stock and density of northern boreal and temperate forests. *Glob. Ecol. Biogeogr.* **2014**, *23*, 297–310. [CrossRef]
11. Barredo, J.I.; San Miguel, J.; Caudullo, G.; Busetto, L. *A European Map of Living Biomass and Carbon Stock*; Executive Report; The Publications Office of the European Union: Luxembourg, 2012; p. 12. [CrossRef]
12. Gallaun, H.; Zanchi, G.; Nabuurs, G.J.; Hengeveld, G.; Schardt, M.; Verkerk, P.J. EU-wide maps of growing stock and above-ground biomass in forests based on remote sensing and field measurements. *For. Ecol. Manag.* **2010**, *260*, 252–261. [CrossRef]
13. Kindermann, G.E.; McCallum, I.; Fritz, S.; Obersteiner, M. A global forest growing stock, biomass and carbon map based on FAO statistics. *Silva Fenn.* **2008**, *42*, 387–396. [CrossRef]
14. Baccini, A.; Goetz, S.J.; Walker, W.S.; Laporte, N.T.; Sun, M.; Sulla-Menashe, D.; Hackler, J.; Beck, P.S.A.; Dubayah, R.; Friedl, M.A.; et al. Estimated carbon dioxide emissions from tropical deforestation improved by carbon-density maps. *Nat. Clim. Chang.* **2012**, *2*, 182. [CrossRef]
15. Santoro, M. *GlobBiomass-Global Datasets of Forest Biomass*; PANGAEA: Bremen, Germany, 2018.

16. Avitabile, V.; Pilli, R.; Camia, A. *The Biomass of European Forests*; EUR 30462 EN; Publications Office of the European Union: Luxembourg, 2020; ISBN 978-92-76-26100-1. [CrossRef]
17. Santoro, M.; Cartus, O.; Carvalhais, N.; Rozendaal, D.M.A.; Avitabile, V.; Araza, A.; De Bruin, S.; Herold, M.; Quegan, S.; Rodríguez-Veiga, P.; et al. The global forest above-ground biomass pool for 2010 estimated from high-resolution satellite observations. *Earth Syst. Sci. Data* **2021**, *13*, 3927–3950. [CrossRef]
18. D'Amico, G.; Vangi, E.; Francini, S.; Giannetti, F.; Nicolaci, A.; Travaglini, D.; Massai, L.; Giambastiani, Y.; Terranova, C.; Chirici, G. Are We Ready for a Web-Based National Forest Information System? State of the Art of for-Est Maps and Airborne Laser Scanning Data Availability in Italy. *IForest* **2021**, *14*, 144–154. [CrossRef]
19. Giannetti, F.; Pegna, R.; Francini, S.; McRoberts, R.E.; Travaglini, D.; Marchetti, M.; Mugnozza, G.S.; Chirici, G. A new method for automated clearcut disturbance detection in Mediterranean coppice forests using Landsat time series. *Remote Sens.* **2020**, *12*, 3720. [CrossRef]
20. ICPP 2019 the Refinement to the 2006 IPCC Guidelines for National Greenhouse Gas Inventories. *Fundam. Appl. Climatol.* **2019**, *2*, 5–13. [CrossRef]
21. FAO; UEP. *The State of the World's Forests 2020. Forests, Biodiversity and People*; FAO: Rome, Italy; UEP: Luxembourg, 2020; ISBN 978-92-5-132419-6.
22. Forest Europe; FAO, U. State of Europe's Forests 2020. In Proceedings of the Ministerial Conference on the Protection of Forests in Europe-Forest Europe, Bratislava, Slovakia, 28–29 2020.
23. Chirici, G.; Giannetti, F.; McRoberts, R.E.; Travaglini, D.; Pecchi, M.; Maselli, F.; Chiesi, M.; Corona, P. Wall-to-wall spatial prediction of growing stock volume based on Italian National Forest Inventory plots and remotely sensed data. *Int. J. Appl. Earth Obs. Geoinf.* **2020**, *84*, 101959. [CrossRef]
24. Kangas, A.; Astrup, R.; Breidenbach, J.; Fridman, J.; Gobakken, T.; Korhonen, K.T.; Maltamo, M.; Nilsson, M.; Nord-Larsen, T.; Næsset, E.; et al. Remote sensing and forest inventories in Nordic countries–roadmap for the future. *Scand. J. For. Res.* **2018**, *33*, 397–412. [CrossRef]
25. White, J.C.; Tompalski, P.; Vastaranta, M.; Wulder, M.A.; Saarinen, N.; Stepper, C.; Coops, N.C. *A Model Development and Application Guide for Generating an Enhanced Forest Inventory Using Airborne Laser Scanning Data and an Area-Based Approach*; Government of Canada: Ottawa, ON, Canada, 2017; ISBN 9780660097381.
26. Vangi, E.; D'amico, G.; Francini, S.; Giannetti, F.; Lasserre, B.; Marchetti, M.; McRoberts, R.E.; Chirici, G. The effect of forest mask quality in the wall-to-wall estimation of growing stock volume. *Remote Sens.* **2021**, *13*, 1038. [CrossRef]
27. Rees, W.G.; Tomaney, J.; Tutubalina, O.; Zharko, V.; Bartalev, S. Estimation of boreal forest growing stock volume in russia from sentinel-2 msi and land cover classification. *Remote Sens.* **2021**, *13*, 4483. [CrossRef]
28. Hawryło, P.; Francini, S.; Chirici, G.; Giannetti, F.; Parkitna, K.; Krok, G.; Mitelsztedt, K.; Lisańczuk, M.; Stereńczak, K.; Ciesielski, M.; et al. The Use of Remotely Sensed Data and Polish NFI Plots for Prediction of Growing Stock Volume Using Di ff erent Predictive Methods. *Remote Sens.* **2020**, *12*, 3331. [CrossRef]
29. Gao, T.; Zhu, J.J.; Yan, Q.L.; Deng, S.Q.; Zheng, X.; Zhang, J.X.; Shang, G.D. Mapping growing stock volume and biomass carbon storage of larch plantations in Northeast China with L-band ALOS PALSAR backscatter mosaics. *Int. J. Remote Sens.* **2018**, *39*, 7978–7997. [CrossRef]
30. Santoro, M.; Cartus, O.; Fransson, J.E.S.; Shvidenko, A.; McCallum, I.; Hall, R.J.; Beaudoin, A.; Beer, C.; Schmullius, C. Estimates of forest growing stock volume for sweden, central siberia, and québec using envisat advanced synthetic aperture radar backscatter data. *Remote Sens.* **2013**, *5*, 4503–4532. [CrossRef]
31. Hauglin, M.; Rahlf, J.; Schumacher, J.; Astrup, R.; Breidenbach, J. Large scale mapping of forest attributes using heterogeneous sets of airborne laser scanning and National Forest Inventory data. *For. Ecosyst.* **2021**, *8*, 65. [CrossRef]
32. Chirici, G.; Chiesi, M.; Fibbi, L.; Giannetti, F.; Corona, P.; Maselli, F. High spatial resolution modelling of net forest carbon fluxes based on ground and remote sensing data. *Agric. For. Meteorol.* **2022**, *316*, 108866. [CrossRef]
33. Huang, S.; Ramirez, C.; Conway, S.; Kennedy, K.; Kohler, T.; Liu, J. Mapping site index and volume increment from forest inventory, landsat, and ecological variables in Tahoe national forest, California, USA. *Can. J. For. Res.* **2017**, *47*, 113–124. [CrossRef]
34. Liu, L. Opportunities of Mapping Forest Carbon Stock and its Annual Increment Using Landsat Time-Series Data. *Geoinform. Geostat. Overv.* **2016**, *4*, 2–5. [CrossRef]
35. Waser, L.T.; Ginzler, C.; Rehush, N. Wall-to-Wall tree type mapping from countrywide airborne remote sensing surveys. *Remote Sens.* **2017**, *9*, 766. [CrossRef]
36. Senf, C.; Pflugmacher, D.; Hostert, P.; Seidl, R. Using Landsat time series for characterizing forest disturbance dynamics in the coupled human and natural systems of Central Europe. *ISPRS J. Photogramm. Remote Sens. Off. Publ. Int. Soc. Photogramm. Remote Sens.* **2017**, *130*, 453–463. [CrossRef]
37. Novo-Fernández, A.; Barrio-Anta, M.; Recondo, C.; Cámara-Obregón, A.; López-Sánchez, C.A. Integration of national forest inventory and nationwide airborne laser scanning data to improve forest yield predictions in north-western Spain. *Remote Sens.* **2019**, *11*, 1693. [CrossRef]
38. Chrysafis, I.; Mallinis, G.; Gitas, I.; Tsakiri-Strati, M. Estimating Mediterranean forest parameters using multi seasonal Landsat 8 OLI imagery and an ensemble learning method. *Remote Sens. Environ.* **2017**, *199*, 154–166. [CrossRef]

39. Chrysafis, I.; Mallinis, G.; Tsakiri, M.; Patias, P. Evaluation of single-date and multi-seasonal spatial and spectral information of Sentinel-2 imagery to assess growing stock volume of a Mediterranean forest. *Int. J. Appl. Earth Obs. Geoinf.* **2019**, *77*, 1–14. [CrossRef]
40. Pascual, A.; Guerra-Hernández, J.; Cosenza, D.N.; Sandoval, V. The role of improved ground positioning and forest structural complexity when performing forest inventory using airborne laser scanning. *Remote Sens.* **2020**, *12*, 413. [CrossRef]
41. Chirici, G.; McRoberts, R.E.; Fattorini, L.; Mura, M.; Marchetti, M. Comparing echo-based and canopy height model-based metrics for enhancing estimation of forest aboveground biomass in a model-assisted framework. *Remote Sens. Environ.* **2016**, *174*, 1–9. [CrossRef]
42. Mura, M.; McRoberts, R.E.; Chirici, G.; Marchetti, M. Estimating and mapping forest structural diversity using airborne laser scanning data. *Remote Sens. Environ.* **2015**, *170*, 133–142. [CrossRef]
43. Montaghi, A.; Corona, P.; Dalponte, M.; Gianelle, D.; Chirici, G.; Olsson, H. Airborne laser scanning of forest resources: An overview of research in Italy as a commentary case study. *Int. J. Appl. Earth Obs. Geoinf.* **2013**, *23*, 288–300. [CrossRef]
44. INFC Italian Forests. *Selected Results of the Third National Forest Inventory. INFC 2015. Carabinieri Command of Forestry, Environmental and Agri-Food Units and CREA-Research Centre for Forestry and Wood*; Tipografia: Trento, Italy, 2021; ISBN 978-88-338-5140-2.
45. Gasparini, P.; Di Cosimo, L.; Floris, A.; De Laurentis, D. *Italian National Forest Inventory—Methods and Results of the Third Survey*; Springer: Berlin/Heidelberg, Germany, 2022; ISBN 9783030986773.
46. Barbati, A.; Marchetti, M.; Chirici, G.; Corona, P. European Forest Types and Forest Europe SFM indicators: Tools for monitoring progress on forest biodiversity conservation. *For. Ecol. Manag.* **2014**, *321*, 145–157. [CrossRef]
47. Giannetti, F.; Barbati, A.; Mancini, L.D.; Travaglini, D.; Bastrup-Birk, A.; Canullo, R.; Nocentini, S.; Chirici, G. European Forest Types: Toward an automated classification. *Ann. For. Sci.* **2018**, *75*, 6. [CrossRef]
48. Bologna, S.; Chirici, G.; Corona, P.; Marchetti, M.; Pugliese, A.; Munafò, M. *Sviluppo e implementazione del IV livello Corine Land Cover per i territori boscati e ambienti semi-naturali in Italia*; Paper Presented at the Annual Meeting for the Society of ASITA; 8a Conferenza Nazionale ASITA: Roma, Italy, 2004; pp. 467–472.
49. Federici, S.; Vitullo, M.; Tulipano, S.; De Lauretis, R.; Seufert, G. An approach to estimate carbon stocks change in forest carbon pools under the UNFCCC: The Italian case. *IForest* **2008**, *1*, 86–95. [CrossRef]
50. McRoberts, R.E.; Næsset, E.; Gobakken, T. The effects of temporal differences between map and ground data on map-assisted estimates of forest area and biomass. *Ann. For. Sci.* **2016**, *73*, 839–847. [CrossRef]
51. INFC Il disegno di campionamento. Inventario Nazionale delle Foreste e dei Serbatoi Forestali di Carbonio. MiPAF-Direzione Generale per le Risorse Forestali Montane e Idriche, Corpo Forestale dello Stato, ISAFA, Trento. 36p. Available online: http://www.isafa.it/scientifica/2004 (accessed on 1 March 2021).
52. Tabacchi, G.; Di Cosmo, L.; Gasparini, P.; Morelli, S. *Stima del Volume e Della Fitomassa Delle Principali Specie Forestali Italiene, Equazioni di Previsione, Tavole del Volume e Tavole Della Fitomassa Arborea Epigea*; Consiglio per la Ricerca e la sperimentazione in Agricoltura, Unità di Ricerca per il monitoraggio e la pianificazione Forestale: Trento, Italy, 2011; ISBN 9788897081111.
53. Borghetti, M.; Chirici, G. Raw data from the Italian National Forest Inventory are on-line and publicly available. *For. Riv. Selvic. Ecol. For.* **2016**, *13*, 33–34. [CrossRef]
54. Tabacchi, G.; De Natale, F.; Di Cosmo, L.; Floris, A.; Gagliano, C.; Gasparini, P.; Genchi, L.; Scrinzi, G.; Tosi, V. *Le stime di superficie 2005-Prima parte. Inventario Nazionale delle Foreste e dei Serbatoi Forestali di Carbonio*; MiPAF – Corpo Forestale dello Stato - Ispettorato Generale, CRA -ISAFA: Trento, Italy, 2007.
55. Maselli, F.; Papale, D.; Puletti, N.; Chirici, G.; Corona, P. Combining remote sensing and ancillary data to monitor the gross productivity of water-limited forest ecosystems. *Remote Sens. Environ.* **2009**, *113*, 657–667. [CrossRef]
56. Chirici, G.; Chiesi, M.; Corona, P.; Puletti, N.; Mura, M.; Maselli, F. Prediction of forest NPP in Italy by the combination of ground and remote sensing data. *Eur. J. For. Res.* **2015**, *134*, 453–467. [CrossRef]
57. Neeti, N.; Kennedy, R. Comparison of national level biomass maps for conterminous US: Understanding pattern and causes of differences. *Carbon Balance Manag.* **2016**, *11*, 19. [CrossRef]
58. Araza, A.; de Bruin, S.; Herold, M.; Quegan, S.; Labriere, N.; Rodriguez-Veiga, P.; Avitabile, V.; Santoro, M.; Mitchard, E.T.A.; Ryan, C.M.; et al. A comprehensive framework for assessing the accuracy and uncertainty of global above-ground biomass maps. *Remote Sens. Environ.* **2022**, *272*, 112917. [CrossRef]
59. Zhang, Y.; Liang, S.; Yang, L. A Review of Regional and Global Gridded Forest Biomass Datasets. *Remote Sens.* **2019**, *11*, 2744. [CrossRef]
60. Huang, W.; Swatantran, A.; Johnson, K.; Duncanson, L.; Tang, H.; Dunne, J.O.N.; Hurtt, G.; Dubayah, R. Local discrepancies in continental scale biomass maps: A case study over forested and non-forested landscapes in Maryland, USA. *Carbon Balance Manag.* **2015**, *10*, 19. [CrossRef]
61. Francini, S.; McRoberts, R.E.; Giannetti, F.; Marchetti, M.; Scarascia-Mugnozza, G.; Chirici, G. The Three Indices Three Dimensions algorithm (3I3D): A new method for forest disturbance mapping and area estimation based on optical remotely sensed imagery. *Int. J. Remote Sens.* **2021**, *42*, 4693–4711. [CrossRef]
62. Urbazaev, M.; Thiel, C.; Cremer, F.; Dubayah, R.; Migliavacca, M.; Reichstein, M.; Schmullius, C. Estimation of forest aboveground biomass and uncertainties by integration of field measurements, airborne LiDAR, and SAR and optical satellite data in Mexico. *Carbon Balance Manag.* **2018**, *13*, 5. [CrossRef]

63. Avitabile, V.; Herold, M.; Henry, M.; Schmullius, C. Mapping biomass with remote sensing: A comparison of methods for the case study of Uganda. *Carbon Balance Manag.* **2011**, *6*, 7. [CrossRef]
64. Puletti, N.; Bascietto, M. Towards a tool for early detection and estimation of forest cuttings by remotely sensed data. *Land* **2019**, *8*, 58. [CrossRef]
65. Francini, S.; McRoberts, R.E.; D'Amico, G.; Coops, N.C.; Hermosilla, T.; White, J.C.; Wulder, M.A.; Marchetti, M.; Mugnozza, G.S.; Chirici, G. An open science and open data approach for the statistically robust estimation of forest disturbance areas. *Int. J. Appl. Earth Obs. Geoinf.* **2022**, *106*, 102663. [CrossRef]
66. Giannetti, F.; Pecchi, M.; Travaglini, D.; Saverio, F.; Amico, G.D.; Vangi, E.; Cocozza, C.; Chirici, G. Estimating VAIA windstorm damaged forest area in Italy using time series Sentinel-2 imagery and continuous change detection algorithms. *Forests* **2021**, *12*, 680. [CrossRef]
67. Bonannella, C.; Chirici, G.; Travaglini, D.; Pecchi, M.; Vangi, E.; D'amico, G.; Giannetti, F. Characterization of Wildfires and Harvesting Forest Disturbances and Recovery Using Landsat Time Series: A Case Study in Mediterranean Forests in Central Italy. *Fire* **2022**, *5*, 68. [CrossRef]
68. Forest Europe. State of Europe's Forests 2015. In Proceedings of the Ministerial Conference on the Protection of Forests in Europe-Forest Europe, Madrid, Spain, 20–2015.
69. *FAO Global Forest Resources Assessment 2015*; FAO: Rome, Italy, 2015; ISBN 9789251088210.